Polymer Chemistry

Efficient detection of polymeric mechanoradicals via fluorescent molecular probes stabilized by steric hindrance

Journal:	*Polymer Chemistry*
Manuscript ID	PY-COM-03-2023-000296.R1
Article Type:	Communication
Date Submitted by the Author:	27-Apr-2023
Complete List of Authors:	Yamamoto, Takumi; Tokyo Institute of Technology, Department of Chemical Science and Engineering Otsuka, Hideyuki; Tokyo Institute of Technology, Department of Chemical Science and Engineering

COMMUNICATION

Efficient detection of polymeric mechanoradicals via fluorescent molecular probes stabilized by steric hindrance

Takumi Yamamoto[a] and Hideyuki Otsuka*[a,b]

Received 00th January 20xx,
Accepted 00th January 20xx

DOI: 10.1039/x0xx00000x

This communication reports the molecular design of fluorescent radical precursors to improve the detectability of polymeric mechanoradicals. The introduction of bulky substituents to the aromatic rings of diarylacetonitrile derivatives significantly improves the ability to detect mechanoradicals.

It is well established that the mechanical degradation of polymers causes main-chain scission, generating free radicals known as mechanoradicals.[1] As early as 1930, Staudinger and co-workers ball-milled high-molecular-weight polystyrene (PS) and observed a decrease in its average molecular weight.[2,3] The involvement of homolytic cleavage of covalent C–C bonds along the polymer backbone under mechanical stress was later experimentally demonstrated by Sohma and co-workers using electron paramagnetic resonance (EPR).[4] This pioneering research has revealed that the evaluation of polymeric mechanoradicals is essential for the analysis of mechanical degradation. Many studies have been performed to detect mechanoradicals in solution using spin-trapping agents, such as nitroso and nitrone compounds,[5–7] and 2,2'-diphenyl-1-picrylhydrazyl (DPPH).[8,9] Despite these recent advances, mechanoradicals are usually unstable at room temperature, making it difficult to qualitatively and quantitatively analyze the short-lived radicals in the solid state. To overcome this problem, several molecular probes capable of visualizing mechanoradicals in the solid state have recently been reported, such as turn-on-type fluorescent radical probes[10–12] and radical-transfer-type fluorescent molecular probes (Fig. 1a).[13–15] To enhance the utility of such fluorescent molecular probes, it is necessary to develop molecular designs for the efficient detection of polymeric mechanoradicals based on existing molecular probes.

Diarylacetonitrile (DAAN) derivatives, which are radical-transfer-type molecular probes, react with highly reactive mechanoradicals to generate the corresponding DAAN radicals. DAAN radicals are relatively stable under atmospheric conditions and fluorescent under UV irradiation,[16–20] allowing a complementary assessment of the polymer main-chain scission via fluorescence intensity and EPR measurements. However, given that the DAAN radicals are metastable radicals,[21] coupling reactions between radicals inevitably reduce the detectability of the polymeric mechanoradicals. Therefore, suppression of such coupling reactions would lead to increased detectability. To implement this idea, we focused on the tertiary butyl (^{t}Bu) group as a bulky substituent. The ^{t}Bu group has long been used in radical chemistry for kinetic stabilization;[22] however, the introduction of bulky substituents to DAAN derivatives can inhibit hydrogen-atom-transfer (HAT) reactions.

In this study, we systematically investigated the effect of steric hindrance in DAAN derivatives with ^{t}Bu groups on their ability to detect mechanoradicals (Fig. 1b). Using the developed molecular probes, we also attempted to detect mechanoradicals in polycarbonate (PC) derived from bisphenol A, which is an engineering plastic known for its high impact resistance.[23] This

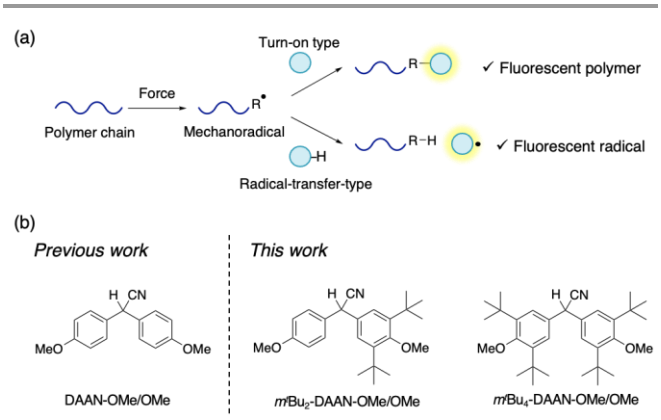

Fig. 1 (a) Schematic illustration of polymeric-mechanoradical detection methods. (b) Chemical structures of **DAAN-OMe/OMe** (previously reported), ***m*^{t}Bu$_2$-DAAN-OMe/OMe**, and ***m*^{t}Bu$_4$-DAAN-OMe/OMe**.

[a] *Department of Chemical Science and Engineering, Tokyo Institute of Technology, 2-12-1 Ookayma, Meguro-ku, Tokyo 152-8550, Japan. E-mail: otsuka@mac.titech.ac.jp*
[b] *Living Systems Materialogy (LiSM) Research Group, International Research Frontiers Initiative (IRFI), Tokyo Institute of Technology, 4259 Nagatsuta-cho, Midori-ku, Yokohama 226-8501, Japan.*
† Electronic supplementary information (ESI) available. See DOI: 10.1039/x0xx00000x

molecular design can be easily adapted to other radical-transfer-type fluorescent radical probes. Furthermore, with just a small quantity of these probes, we can readily apply this technique to detect mechanical damage in polymeric materials.

DAAN-OMe/OMe was synthesized according to a literature procedure (Scheme S1),[24] while ***m*^{t}Bu$_2$-DAAN-OMe/OMe** and ***m*^{t}Bu$_4$-DAAN-OMe/OMe** were synthesized in two or three steps from commercially available precursors with reference to the literatures (Scheme S2–S5).[24,25] The chemical structures of the DAAN derivatives were fully characterized using ^{1}H and ^{13}C NMR as well as FT-IR spectroscopy in combination with mass-spectrometry measurements (Figs. S1–S7).

To evaluate the ability of the probes to detect polymeric mechanoradicals, ball-milling experiments were carried out using a Retch MM400 mixer mill (10-mL stainless-steel milling jar using one 5-mm-diameter stainless-steel ball). For that purpose, PS (100 mg) was ball-milled at 30 Hz for 10–30 min in the presence of each DAAN derivative (39 μmol). The number-average molecular weight (M_n) and the polydispersity (M_w/M_n) of the mixtures of polystyrene and ***m*^{t}Bu$_4$-DAAN-OMe/OMe** before and after ball-milling are summarized in Fig. 2a. After the ball-milling test, M_n decreased and M_w/M_n increased, indicating that polymer degradation had occurred. In addition, the emission of fluorescence by the samples after ball-milling could be observed under UV irradiation (λ_{ex} = 365 nm) (Fig. 2b).

To confirm that radical transfer from the polymeric mechanoradicals to the DAAN moieties occurred, fluorescence spectroscopy and EPR measurements were conducted. Fig. 2c shows the normalized fluorescence spectra of the DAAN derivatives after the ball-milling (The original fluorescence spectra can be found in Fig. S8). Compared with that of **DAAN-OMe/OMe** radicals, the ***m*^{t}Bu$_2$-DAAN-OMe/OMe** and ***m*^{t}Bu$_4$-DAAN-OMe/OMe** radicals exhibit red-shifted emission (**DAAN-OMe/OMe**: λ_{em} = 555 nm; ***m*^{t}Bu$_2$-DAAN-OMe/OMe**: λ_{em} = 568 nm; ***m*^{t}Bu$_4$-DAAN-OMe/OMe**: λ_{em} = 583 nm). To understand the fluorescence properties of the DAAN radicals, we performed density-functional-theory (DFT) and time-dependent (TD)-DFT calculations at the unrestricted M06-2X level with the 6-311+G(d,p) basis set, since it has been reported to demonstrate better agreement with the emission of fluorescent radicals than UB3LYP.[26,27] The vertical emission energies from the optimized lowest doublet excited state (D_1) calculated using TD-DFT were found to be reduced upon introducing the ^{t}Bu group (Tables S1 and S2). This result is consistent with the experimental red-shifted emission upon introducing the ^{t}Bu group. This remarkable red-shifted emission in the DAAN derivatives is probably due to the introduction of the ^{t}Bu group, which causes a significant structural change between the ground and excited states. In fact, comparing the optimized ground doublet state (D_0) with the optimized D_1 state, the dihedral angle decreases in the order **DAAN-OMe/OMe** < ***m*^{t}Bu$_2$-DAAN-OMe/OMe** < ***m*^{t}Bu$_4$-DAAN-OMe/OMe** (Table S3).

As shown in Fig. 2d, the EPR measurements clearly demonstrate signals originating from the generation of a radical species after the ball-milling. The *g* values (2.003) of the observed signals indicate that they originate from carbon-centered radicals. To investigate whether the carbon-centered radicals were thermally generated or not, EPR measurements were conducted at 100 °C on i) DAAN derivatives, ii) PS, and

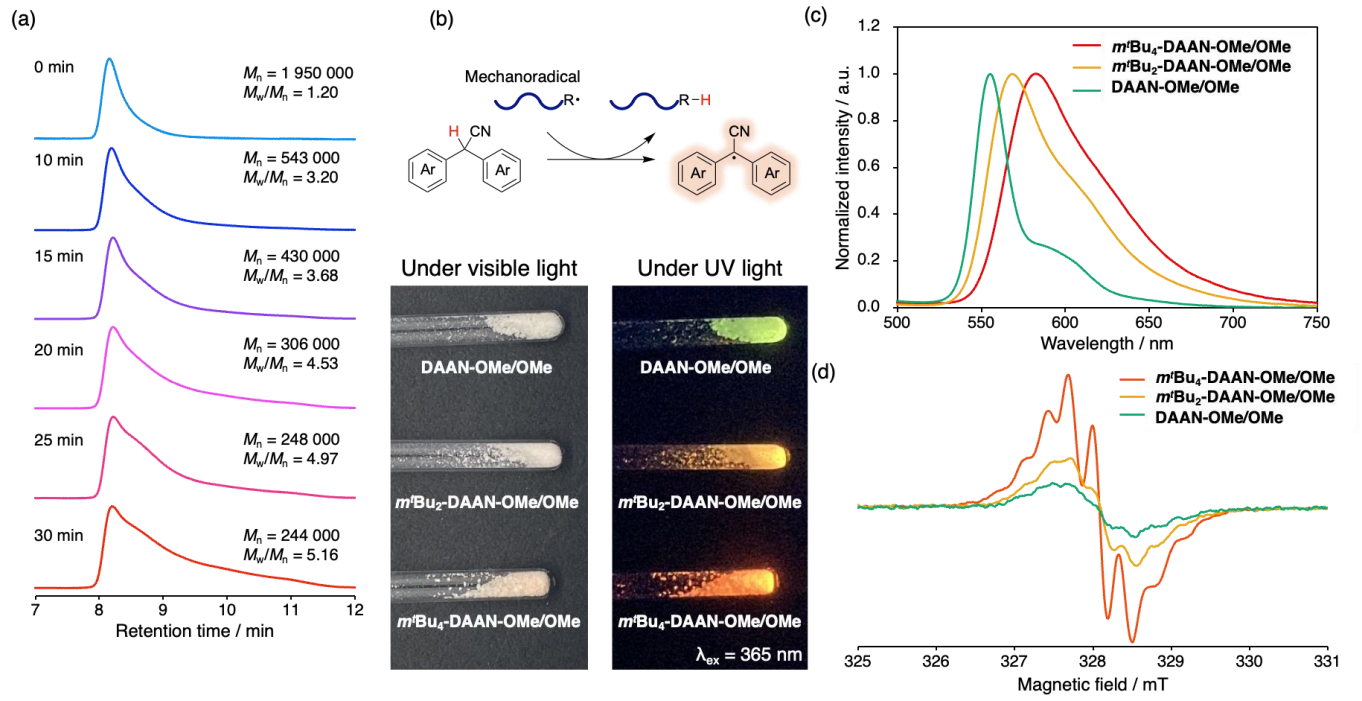

Fig. 2 GPC curves of mixtures of polystyrene (M_n = 1 950 000; M_w/M_n = 1.20) and ***m*^{t}Bu$_4$-DAAN-OMe/OMe** (39 μmol) before and after ball-milling. Data refer to sample subjected to mechanical processing at a milling frequency of approximately 30.0 Hz. (b) Photographs of the mixtures of polystyrene (M_n = 1 950 000; M_w/M_n = 1.20) and DAAN derivatives (39 μmol) after ball-milling under visible right (left) and UV (λ_{ex} = 365 nm) irradiation (right). (c) Fluorescence spectra (λ_{ex} = 365 nm) and (d) ESR spectra of the mixtures of polystyrene (M_n = 1 950 000; M_w/M_n = 1.20) and DAAN derivatives (39 μmol) after ball-milling (30 min).

iii) the mixtures of DAAN derivatives and PS. Furthermore, to demonstrate that DAAN radicals are generated through a radical-transfer reaction from mechanoradicals, similar ball-milling tests were carried out using DAAN derivatives alone. As shown in Figs. S9 and S10, signals assignable to carbon-centered radicals were hardly observed in these cases. These results suggest that the mechanically induced HAT reaction proceeded normally, even once ^{t}Bu groups had been introduced on the aromatic rings of the DAAN skeleton. The amount of DAAN radicals generated in the ball-milling tests of the mixtures of PS and the DAAN derivatives were estimated based on EPR measurements by comparing the integration area of each spectrum with that of a solution of 4-hydroxy-2,2,6,6-tetramethylpiperidin-1-oxyl (TEMPOL) as a standard. The results confirmed that the introduction of the ^{t}Bu groups into the DAAN derivatives increases the amount of DAAN radicals detectable by EPR measurement (Fig. 3a). Compared with **DAAN-OMe/OMe**, the ability of ***m*^{t}Bu$_2$-DAAN-OMe/OMe** and ***m*^{t}Bu$_4$-DAAN-OMe/OMe** to detect mechanoradicals were 1.8 and 3.6 times greater, respectively. The increase in the conversion should be attributed to inhibition of the coupling reaction between the radicals by the bulky substituents. In fact, the decay of the radical intensity after ball-milling was evaluated using time-dependent EPR and fluorescence-spectroscopy measurements and showed that the introduction of the ^{t}Bu groups significantly reduces the radical deactivation and extinction of fluorescence (Figs. 3b, 3c). Furthermore, when observing the samples after 96 hours, it was found that **DAAN-OMe/OMe** had almost completely lost its original fluorescence, whereas ***m*^{t}Bu$_4$-DAAN-OMe/OMe** still exhibited strong fluorescence emission (Fig. S11). In addition to evaluating the specific steric hindrance of the radicals, the percentage of buried volume (%V_{Bur}) was calculated.[28] Specifically, a sphere was set up with the carbon-centered radical at the origin and a radius of 6 Å; these dimensions are the most suitable to consider the spatial steric protection of the radical by the surrounding atoms (Fig. 3d).[29] The buried volumes and steric maps presented in this work were obtained using the SambVca 2 Web application.[30] The topography indicates that the ^{t}Bu groups of the ***m*^{t}Bu$_2$-DAAN-OMe/OMe** and ***m*^{t}Bu$_4$-DAAN-OMe/OMe** radicals protect the carbon-centered radicals well, and that the steric hindrance of the ***m*^{t}Bu$_4$-DAAN-OMe/OMe** (%V_{Bur} = 40.7) radical is higher than that of the **DAAN-OMe/OMe** (%V_{Bur} = 26.5) and ***m*^{t}Bu$_2$-DAAN-OMe/OMe** (%V_{Bur} = 34.3) radicals, which was attributed to the presence of more ^{t}Bu groups (Fig. 3e). Both experimental and computational results suggest that the introduction of the ^{t}Bu group improves the mechanoradical detectability due to the steric protection of the carbon-centered radicals.

Finally, the same ball-milling test was performed using PC, which is one of the most widely used engineering plastics. PC (M_n = 37 kg mol^{-1}; M_w/M_n = 2.02, 100 mg) was ball-milled at 30 Hz for 30 min in the presence of each DAAN derivative (39

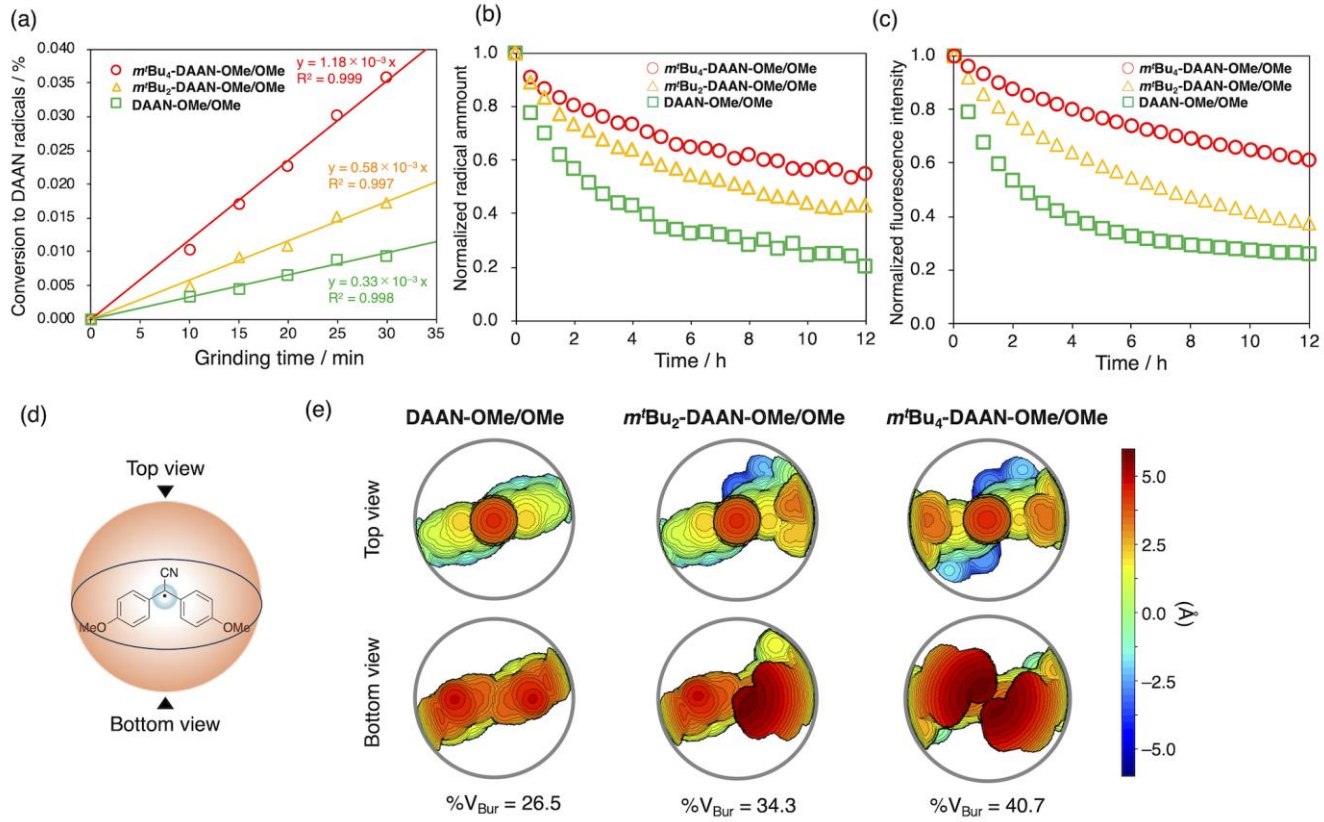

Fig. 3 (a) Conversion of the DAAN derivatives into the corresponding DAAN radicals estimated based on EPR measurements. (b) Time-dependent normalized amount of DAAN radicals calculated from EPR measurements under atmospheric conditions. (c) Time-dependent normalized fluorescence intensity calculated from EPR measurements under atmospheric conditions. (d) 3D sphere display of the steric descriptor of the buried volume (%V_{Bur}). (e) Steric maps of a series of DAAN radicals.

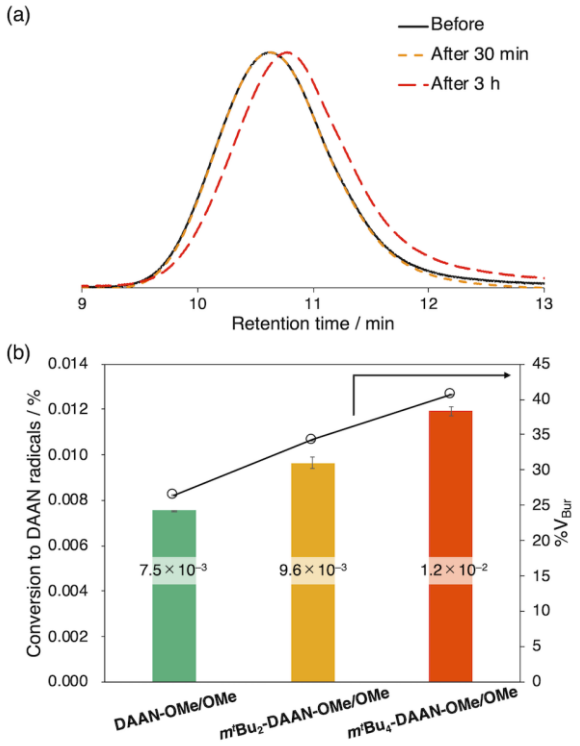

Fig. 4 (a) GPC curves of the mixtures of polycarbonate (M_n = 37 000; M_w/M_n = 2.02) and ***m*'Bu$_4$-DAAN-OMe/OMe** (39 μmol) before and after ball-milling. (b) Conversion of the DAAN derivatives to the corresponding DAAN radicals estimated based on EPR measurements, and the percentages of buried volume (%V_{Bur}).

μmol). After ball-milling for 30 min, no significant decrease in molecular weight could be detected using gel-permeation chromatography (GPC) (Fig. 4a), even though we succeeded in detecting the generation of mechanoradicals using the DAAN derivatives (Fig. 4b). EPR measurements were conducted at 100°C on PC and the mixtures of DAAN derivatives and PC, but no radical species were observed (Fig. S12). On the other hand, after grinding only PC for 3 hours, a decrease in molecular weight was slightly observed (Fig. 4a). These results indicate that polymer chain of PC surely cleaved by mechanical stress and even initial minimal polymer-chain scission that cannot be observed using GPC can be detected using this method. Furthermore, the ability to detect mechanoradical followed the order **DAAN-OMe/OMe** < ***m*'Bu$_2$-DAAN-OMe/OMe** < ***m*'Bu$_4$-DAAN-OMe/OMe**, as was the case with PS. It can thus be feasibly expected that this method will be applied in the near future to the detection of mechanoradicals generated during the processing and forming of polymers and the degradation of practical materials.

In summary, the radical-transfer-type fluorescent molecular probes ***m*'Bu$_2$-DAAN-OMe/OMe** and ***m*'Bu$_4$-DAAN-OMe/OMe** were prepared and compared with **DAAN-OMe/OMe**. We successfully improved the ability of DAAN derivatives to detect mechanoradicals via the steric protection of the carbon-centered radicals. At present, we attribute this improved mechanoradical-detection ability to the presence of the bulky substituents, which offer steric protection and thus kinetic stabilization. Due to their high mechanoradical-detection ability, the DAAN derivatives can detect polymer-chain scission that is difficult to detect using GPC. Comprehensive experiments to detect mechanoradicals generated in more practical materials are currently in progress in our laboratory.

Author contributions

T.Y., and H.O. conceived the concept, designed the experiments. T.Y. performed the experiments and analyzed the data. T.Y., and H.O. wrote the manuscript.

Conflicts of interest

There are no potential conflicts of interest to declare.

Acknowledgements

This work was supported by KAKENHI grants 21H04689 (H.O.) from the Japan Society for the Promotion of Science (JSPS), JSPS Research fellowships for Young Scientists 22J21853 (T.Y.), the ANRI Fellowship (T.Y.) and JST CREST (grant JPMJCR1991 to H.O.). The numerical calculations were carried out on the TSUBAME3.0 supercomputer at the Tokyo Institute of Technology supported by the MEXT Project of the Tokyo Tech Academy for Convergence of Materials and Informatics (TAC-MI).

Notes and references

1 R. Boulatov, *Polymer Mechanochemistry*, 2016, vol. 53.
2 H. Staudinger and E. O. Leupold, *Ber. Dtsch. Chem. Ges. B*, 1930, **63**, 730–733.
3 H. Staudinger and W. Heuer, *Ber. Dtsch. Chem. Ges. B*, 1934, **67**, 1159–1164.
4 J. Sohma, *Prog. Polym. Sci.*, 1989, **14**, 451–596.
5 T. Hayashi, K. Kinashi, W. Sakai, N. Tsutsumi, A. Fujii, S. Inada and H. Yamamoto, *Polymer*, 2021, **217**, 123416.
6 M. Sono, K. Kinashi, W. Sakai and N. Tsutsumi, *Macromolecules*, 2017, **50**, 254–263.
7 F. Wang, M. Burck and C. E. Diesendruck, *ACS Macro Lett.*, 2017, **6**, 42–45.
8 M. M. Caruso, D. A. Davis, Q. Shen, S. A. Odom, N. R. Sottos, S. R. White and J. S. Moore, *Chem. Rev.*, 2009, **109**, 5755–5798.
9 N. Willis-Fox, E. Rognin, C. Baumann, T. A. Aljohani, R. Göstl and R. Daly, *Adv. Funct. Mater.*, 2020, **30**, 2002372.
10 K. Kubota, N. Toyoshima, D. Miura, J. Jiang, S. Maeda, M. Jin and H. Ito, *Angew. Chem., Int. Ed.*, 2021, **60**, 16003–16008.
11 C. Wang, S. Akbulatov, Q. Chen, Y. Tian, C.-L. Sun, M. Couty and R. Boulatov, *Nat. Commun.*, 2022, **13**, 3154.
12 Q. Huang, O. Hassager and J. Madsen, *Macromolecules*, 2022, **55**, 9431–9441.
13 T. Yamamoto, S. Kato, D. Aoki and H. Otsuka, *Angew. Chem., Int. Ed.*, 2021, **60**, 2680–2683.
14 E. Jung, D. Yim, H. Kim, G. I. Peterson and T.-L. Choi, *J. Polym. Sci.*, 2023, **61**, 553–560.
15 T. Yamamoto, D. Aoki and H. Otsuka, *ACS Macro Lett.*, 2021, **10**, 744–748.
16 T. Sumi, R. Goseki and H. Otsuka, *Chem. Commun.*, 2017, **53**, 11885–11888.

17 S. Kato, S. Furukawa, D. Aoki, R. Goseki, K. Oikawa, K. Tsuchiya, N. Shimada, A. Maruyama, K. Numata and H. Otsuka, *Nat. Commun.*, 2021, **12**, 126.
18 J. Kida, D. Aoki and H. Otsuka, *Aggregate*, 2021, **2**, e50.
19 Z. Liu, H. K. Bisoyi, Y. Huang, M. Wang, H. Yang and Q. Li, *Angew. Chem., Int. Ed.*, 2022, **61**, e202115755.
20 M. van Galen, J. P. Kaniraj, B. Albada and J. Sprakel, *J. Phys. Chem. C*, 2022, **126**, 1215–1221.
21 K. Kato and A. Osuka, *Angew. Chem., Int. Ed.*, 2019, **58**, 8978–8986.
22 K. Uchida and T. Kubo, *J. Synth. Org. Chem. Japan*, 2016, **74**, 1069–1077.
23 K. Takeuchi, in *Polymer Science: A Comprehensive Reference*, Elsevier, 2012, vol. 5, pp. 363–376.
24 D. K. Singh, S. S. Prasad, J. Kim and I. Kim, *Org. Chem. Front.*, 2019, **6**, 669–673.
25 E. M. Igumnova, E. Mishchenko, T. Haug, H.-M. Blencke, J. U. E. Sollid, E. G. A. Fredheim, S. Lauksund, K. Stensvåg and M. B. Strøm, *Bioorg. Med. Chem.*, 2018, **26**, 4930–4941.
26 S. Sang, F. Chen and C. Zhang, *Int. J. Quant. Chem.*, 2021, **121**, e26522.
27 Y. Zhao and D. G. Truhlar, *Theor. Chem. Acc.*, 2008, **120**, 215–241.
28 G. Luchini and R. Paton, *DBSTEP DFT Based Steric Parameters*, 2022, DOI: 10.5281/zenodo.4702097.
29 X. Wang, P. Xue, C. Zhou, Y. Zhang, P. Li and R. Chen, *J. Mater. Chem. C*, 2022, **10**, 18343–18350.
30 L. Falivene, Z. Cao, A. Petta, L. Serra, A. Poater, R. Oliva, V. Scarano and L. Cavallo, *Nat. Chem.*, 2019, **11**, 872–879.